ELSEVIER

Biochimica et Biophysica Acta 1565 (2002) 232–245

BIOCHIMICA ET BIOPHYSICA ACTA
BBA

www.bba-direct.com

Review

Structural model of the transmembrane F_o rotary sector of H^+-transporting ATP synthase derived by solution NMR and intersubunit cross-linking in situ

Robert H. Fillingame*, Oleg Y. Dmitriev

Department of Biomolecular Chemistry, University of Wisconsin Medical School, 1300 University Avenue, Madison, WI 53706-1532, USA

Received 5 February 2002; received in revised form 16 May 2002; accepted 24 May 2002

Abstract

H^+-transporting, F_1F_o-type ATP synthases utilize a transmembrane H^+ potential to drive ATP formation by a rotary catalytic mechanism. ATP is formed in alternating β subunits of the extramembranous F_1 sector of the enzyme, synthesis being driven by rotation of the γ subunit in the center of the F_1 molecule between the alternating catalytic sites . The H^+ electrochemical potential is thought to drive γ subunit rotation by first coupling H^+ transport to rotation of an oligomeric rotor of *c* subunits within the transmembrane F_o sector. The γ subunit is forced to turn with the *c*-oligomeric rotor due to connections between subunit *c* and the γ and ε subunits of F_1. In this essay we will review recent studies on the *Escherichia coli* F_o sector. The monomeric structure of subunit *c*, determined by NMR, shows that subunit *c* folds in a helical hairpin with the proton carrying Asp^{61} centered in the second transmembrane helix (TMH). A model for the structural organization of the c_{10} oligomer in F_o was deduced from extensive cross-linking studies and by molecular modeling. The model indicates that the H^+-carrying carboxyl of subunit *c* is occluded between neighboring subunits of the c_{10} oligomer and that two *c* subunits pack in a ''front-to-back'' manner to form the H^+ (cation) binding site. In order for protons to gain access to Asp^{61} during the protonation/deprotonation cycle, we propose that the outer, Asp^{61}-bearing TMH-2s of the *c*-ring and TMHs from subunits composing the inlet and outlet channels must turn relative to each other, and that the swiveling motion associated with Asp^{61} protonation/deprotonation drives the rotation of the *c*-ring. The NMR structures of wild-type subunit *c* differs according to the protonation state of Asp^{61}. The idea that the conformational state of subunit *c* changes during the catalytic cycle is supported by the cross-linking evidence in situ, and two recent NMR structures of functional mutant proteins in which critical residues have been switched between TMH-1 and TMH-2. The structural information is considered in the context of the possible mechanism of rotary movement of the c_{10} oligomer during coupled synthesis of ATP.

Keywords: ATP synthase; Proton transport; Rotary motor; Subunit *c*; NMR; F_o structure; Cross-linking; Molecular modeling

1. Introduction

H^+-transporting F_1F_o ATP synthases utilize a transmembrane H^+ electrochemical potential to drive ATP formation via a rotary catalytic mechanism. Closely related enzymes are found in the plasma membrane of eubacteria, the inner membrane of mitochondria, and the thylakoid membrane of chloroplasts [1]. The enzymes are composed of distinct extramembranous and transmembranous sectors, termed F_1 and F_o, respectively. Proton movement through F_o is reversibly coupled to ATP synthesis or hydrolysis in catalytic sites on F_1. Each sector of the enzyme is composed of multiple subunits with the simplest composition being $\alpha_3\beta_3\gamma\delta\varepsilon$ for F_1 and $a_1b_2c_{10}$ for F_o in the case of the *Escherichia coli* enzyme [2,3]. Homologous subunits are found in mitochondria and chloroplasts [1]. Atomic resolution X-ray structures of the $\alpha_3\beta_3\gamma$ and the $\alpha_3\beta_3\gamma\varepsilon$ portion of bovine F_1 shows the three α and three β subunits alternating around a centrally located γ subunit, wherein the γ subunit interacts asymmetrically with the three αβ subunit pairs [4,5][1]. Subunit γ was subsequently shown to rotate within the $\alpha_3\beta_3$ hexamer during catalysis [6–8].

Abbreviations: DCCD, dicyclohexylcarbodiimide; SDS, sodium dodecyl sulfate; TMH, transmembrane helix

* Corresponding author. Tel.: +1-608-262-1439; fax: +1-608-262-5253.
E-mail address: rhfillin@facstaff.wisc.edu (R.H. Fillingame).

[1] The *E. coli* subunit nomenclature is used throughout. The *E. coli* ε subunit is called δ in the mitochondrial nomenclature.

0005-2736/02/$ - see front matter © 2002 Elsevier Science B.V. All rights reserved.
PII: S0005-2736(02)00572-2

Rotation of γ is thought to change the binding affinities in catalytic sites and alternately promote tight substrate binding and then product release during catalysis [9]. The γ and ε subunits interact with each other and are known to rotate as a fixed unit [10,11]. During ATP synthesis, the rotation of γε must be driven by proton flux through F_o. Recent evidence now supports a rotary mechanism for ATP synthesis in which proton-transport coupled rotation of an oligomeric ring of 10 *c* subunits in the membrane is coupled to rotary movement of subunits γε between the alternating catalytic sites [12–15]. In this model, the sequential protonation and deprotonation of Asp^{61} at the center of the second transmembrane helix (TMH) of subunit *c* is coupled with a stepwise movement of the rotor ([16–18]; Fig. 1). Although a detailed structure of the complete F_o complex is not at hand, current structural and biochemical evidence fits well with the rotary hypothesis. Following a brief overview of this evidence, we will focus on the combined use of solution NMR and cross-linking in situ in defining key feature of the oligomeric *c*-ring.

Several experimental approaches have contributed to our present understanding of the structural arrangement of subunit *c* in F_o. Low-resolution electron microscopic and atomic force microscopic images initially suggested a ring-like arrangement of the *c* oligomer with subunits *a* and *b* lying at the periphery of the ring [19–21]. An atomic resolution structure of monomeric subunit *c*, determined by NMR in a membrane-mimetic solvent, is discussed in detail below. In brief, the protein was found to fold as a hairpin of two α helices, packed in parallel and connected by a short polar loop, with the helix–helix interactions in accord with those expected for the protein in the native membrane [22]. The carboxyl side chain of Asp^{61} was packed at the center of the "front" flattened face of the interacting helices. On the basis of the NMR model [22] and distance constraints derived by inter-subunit Cys–Cys cross-linking [23,24], a model for an oligomeric ring of *c* subunits in the membrane was calculated [25]. In the model, the multiple copies of subunit *c* are proposed to be arranged in a cylinder-like structure such that the TMHs form two concentric rings with the N- and C- terminal helices positioned in the inner and outer circle of the ring, respectively. Residues within the polar loops at the top of the cylinder were known to interact with the γ and ε subunits of F_1 in the native enzyme [26,27], and this interaction was modeled on the basis of the NMR and crystal structures of subunit *c* and ε and now the X-ray structure of γε [28–31]. The model for the oligomeric ring of subunit *c* in F_o is now supported by

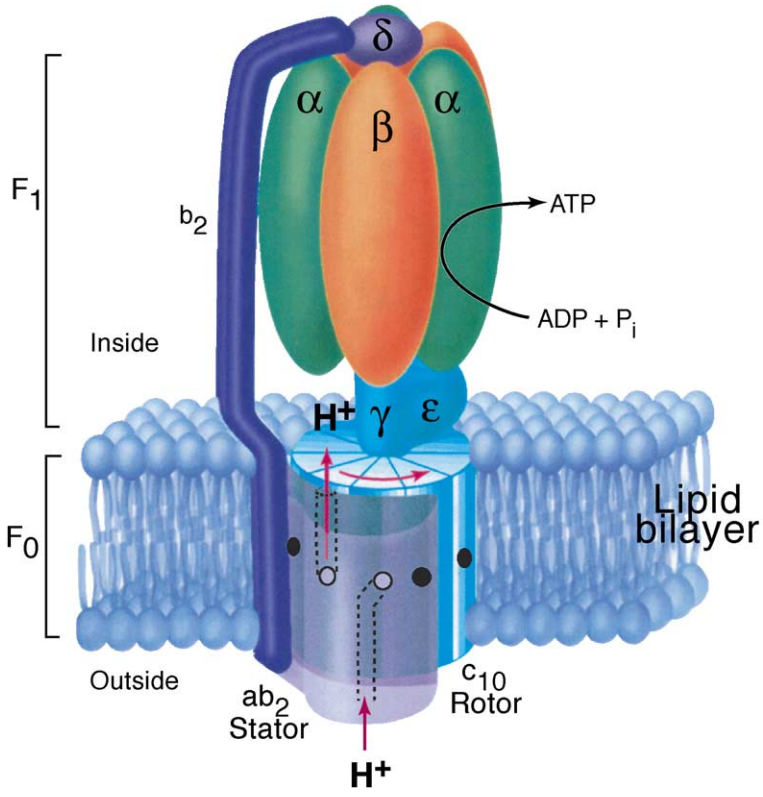

Fig. 1. Rotary model for how *E. coli* F_1F_o ATP synthase catalyzes synthesis of ATP (adapted from Ref. [77]). Rotation of the c_{10} oligomer in the direction indicated is driven by the protonmotive force. Protons enter the assembly through the periplasmic inlet channel and bind to the Asp^{61} carboxylate (open circle). The protonated binding site (filled circle) then moves from the a_1b_2 stator component towards the lipid phase of the membrane where, after 10 steps, it reaches an outlet channel on the cytoplasmic side of the membrane to release the proton. The γ and ε subunits are proposed to remain fixed to the top of one set of *c*-subunits so that rotation of the rotor also drives rotation of subunit γ within the $\alpha_3\beta_3$ subunits of F_1. The b_2 and δ subunits of the stator hold the $\alpha_3\beta_3$ subunits in a fixed position as the γ subunit turns within to drive ATP synthesis.

direct crystallographic observations at 3.9-Å resolution [32]. The number of *c* subunits in the complex is at present the subject of controversy, with numbers in the range of 10–14 being proposed for different species [3,32–34]. We initially favored the number of 12, based upon the expression and cross-linking of active, genetically fused *c* dimers and *c* trimers in *E. coli* [24]. However, we now believe that the preferred number of subunits in the *c*-ring of *E. coli* is 10, based upon coexpression and cross-linking of genetically fused trimers and tetramers into decameric structures [3].

As indicated above, electron and atomic force microscopic images initially suggested a ring-like arrangement of *c* subunits with subunits *a* and *b* placed at the periphery of the ring [19–21]. The placement of subunits *a* and *b* at the outside of the ring is now supported by cross-linking studies [35–37]. Subunit *b* is present in two copies and probably serves as the stalk of the stator holding the $\alpha_3\beta_3$ subunits of F_1 in a fixed position relative to the transmembrane regions of subunits *a* and *b* [38–40]. Electron micrographs now indicate a second stalk at the periphery of the F_1F_o interface which is presumed to represent the b_2 dimer extending from F_o to F_1 [41–43]. The cytoplasmic domain of subunit *b* binds to subunit δ of F_1 in solution [44], and interactions between subunit *b* and subunits δ and α at the top of the F_1 molecule have been demonstrated in F_1F_o [45,46]. To reach the top of the F_1 molecule, subunit *b* is estimated to extend 110 Å from the surface of the membrane [45]. Subunit *b* is anchored in the membrane via a single TMH at the N terminus, the structure of the segment having been determined recently by NMR [36]. The membrane traversing α-helices of the *b* subunits are close enough to each other to be efficiently cross-linked, following genetic introduction of Cys, and the pattern of cross-linking suggests the angle of packing of the two subunit *b* TMHs in F_o [36]. This helix can be cross-linked to *c*TMH-2 and lends support to the idea that subunit *b* packs outside the *c*-ring [47]. Subunit *a* is a highly hydrophobic protein that is known to span the membrane with five TMHs [48–50]. It is presumed to be the major component of the alternate access channels shown in Fig. 1, but the placement of these channels in the protein is not yet determined. Residues in *a*TMH-4 have been implicated in the proton transport mechanism and may provide portions of the access channels from *c*Asp^{61} to the two sides of the membrane. Residue *a*R210 in *a*TMH-4 is proposed to facilitate proton release by lowering the pK_a of Asp^{61} as it passes the *a* subunit of the stator [18,51]. Following introduction of appropriate Cys residues, *a*TMH-4 and *c*TMH-2 can be cross-linked over a membrane spanning length of 19 residues in each helix [35]. Oddly, the face of *c*TMH-2 that cross-links to *a*TMH-4 packs next to *c*TMH-1 in the NMR structure and *c*-ring model [22,25], rather than on the outer surface. Further, in the oligomeric ring model, *c*Asp^{61} is packed between subunits where it would be inaccessible to interaction with *a*R210 [25]. In a more recent NMR structure of subunit *c* [52], solved at pH 8 under conditions where Asp^{61} should be ionized, *c*TMH-2 is rotated by 140° relative to the pH 5 structure where Asp^{61} is fully protonated. The cross-linking results and new NMR structure have led to the suggestions that *c*TMH-2 may rotate during the proton translocation cycle, which would make *c*Asp^{61} accessible to *a*Arg^{210} with the helical rotation in turn driving the stepwise movements of the *c*-ring. The evidence for such a model is considered in the context of the NMR structures in the discussion below.

2. NMR structure of monomeric subunit *c*

The solution structure of monomeric subunit *c* was initially determined in a monophasic chloroform–methanol–water (4:4:1) solvent mixture at pH 5 [22]. The protein folds in a hairpin-like structure of two extended α-helices in the exact manner predicted for native protein inserted in the lipid bilayer of the membrane (Fig. 2). At the apex of the hairpin lie three conserved residues, Arg^{41}–Gln^{42}–Pro^{43}, which from genetic and cross-linking studies are predicted to interact with subunits γ and ε of F_1 [26–28,53,54]. The predicted TMHs (residues 10–31 and 54–76) pack closely over their entire length. Both helices are composed entirely of nonpolar residues with the exception of Asp^{61} in TMH-2. TMH-1 is highly enriched in Gly and Ala residues which predictably results in a smaller cross-sectional diameter. The α-helical structure of TMH-2 is disrupted around Asp^{61} due to interrupted hydrogen bonding at Pro^{64} and the angle of helical packing changes in direction from here to the C terminus. Precise residue-residue proximities, which were predicted for the folded protein in native F_o, are also observed in the NMR structure (Fig. 2). The proximity of Asp^{61} to Ala^{24} had been predicted from aspartyl-interchange mutants, where the essential carboxylate side chain was moved from position 61 on TMH-1 to position 24 on TMH-2 with retention of function [55,56]. In addition, Asp^{61} was predicted to be close to Ala^{24} and Ile^{28} based on the dicyclohexylcarbodiimide (DCCD)-resistance mutations *c*A24S and *c*I28T, which reduce the reactivity of Asp^{61} with DCCD [57]). The proximity of Pro^{64} to Ala^{20} had been predicted from a second site mutation of *c*A20P, which suppressed the nonfunctional *c*P64L and *c*P64A mutations [58,59]. The structure of the P20A64 protein is discussed below.[2] The wild-type protein also folds in the solvent mixture such that the environment around the Asp^{61} carboxylate remains chemically unique. This was indicated by the retention of specificity in the reaction of DCCD with Asp^{61} [60], and by the unusually elevated pK_a of the Asp^{61} carboxyl group [61]. We have suggested that this mixed solvent system, with its polar and nonpolar components, may promote folding of the protein by heterogeneous

[2] In this review we will identify several double mutants of subunit *c* by referring to the residue at the final position only, i.e. A20P/P64A = P20A64, A24D/D61G = D24G61, and A24D/D61N = D24N61.

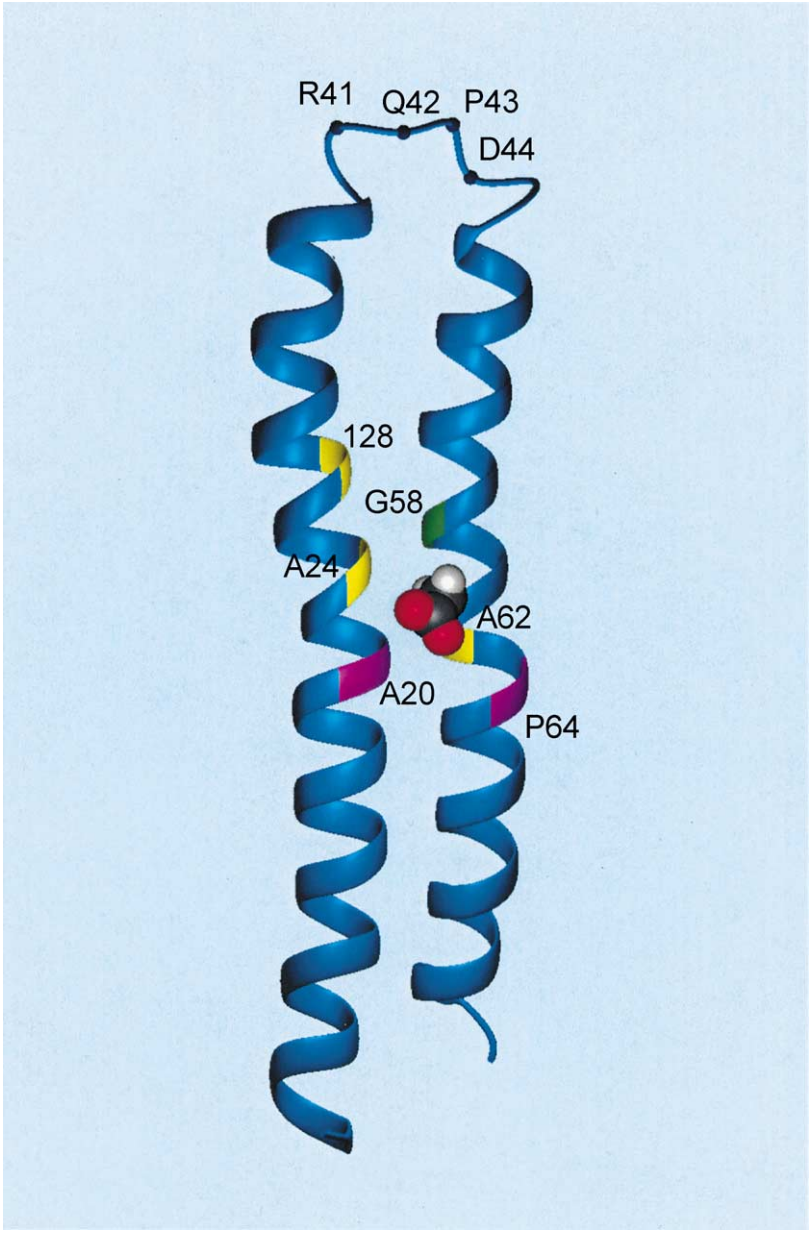

Fig. 2. Hairpin-like folding of subunit *c* in the NMR structure at pH 5 with Asp^{61} protonated [22]. The positions of key residues discussed in the text are indicated. The Asp^{61} side chain packs towards the "front" of the structure and the Ala^{24} and Ile^{28} side chains (not shown) pack towards the "back" of the structure. Structure is depicted from coordinates 1c0v [52].

interactions of the solvent components with the polar and hydrophobic regions of the protein. In this sense, the solvent may function like an amphipathic detergent to solubilize the protein in a folded state.

The high resolution NMR structure did provide one major surprise. The close interactions of TMH-1 and TMH-2 over the length of the structure result in an oval-shaped molecule, when viewed in cross section, with extended flattened surfaces on the two sides of the molecule. The Asp^{61} side chain extends from what we have called the "front" surface (projection indicated in Fig. 2), and the Ala^{24} and Ile^{28} and Ala^{62} side-chains from the "back" surface. These residues had been predicted to interact to form the proton (cation) binding site in the *c*-oligomer of Fo. In order to reconcile the NMR structure with the functional studies, the subunits were proposed to associate in the oligomer with the flattened front face of one subunit packed against the flattened back face of a second subunit to form a functional dimer [22]. Such packing would maximize inter subunit contact. The proposed packing would also explain the following observations: (i) In the functional aspartyl interchange mutants [55,56], where the essential Asp was moved from position 61 to 24, the essential carboxylate would end up in the same cavity between subunits whether it was anchored at backbone position 24 or 61. (ii) In the DCCD-resistant mutants [57], the substituted side chains at

positions 24 or 28 of one monomer would neighbor Asp^{61} of the adjacent monomer and thereby affect reactivity of Asp^{61} with DCCD. (iii) In *E. coli* and *Propiogenium modestum* F_oF_1, several residues have been identified which affect the cation binding selectivity of the essential carboxylate. In the case of the *E. coli* enzyme, the combined substitutions of Val^{60}–Asp^{61}–Ala^{62}–$Ile^{63} \rightarrow Ala^{60}$–$Glu^{61}$–$Ser^{62}$–$Gly^{63}$ around the cation binding site enables Li^+ binding, wherein the $Ala^{62} \rightarrow Ser$ substituted residue was concluded to be critical as a liganding group [62]. The packing of subunits would allow an interaction of the Ser^{62} hydroxyl on the back face of one subunit with the Glu^{61} carboxyl at the front face of a second subunit. A model for this interaction is discussed below. In the case of the *P. modestum* enzyme, the Gln^{32}, Glu^{65} and Ser^{66} side chains (at positions equivalent to 28, 61 and 62, respectively, for the *E. coli* enzyme) are required for Na^+ (Li^+) binding [63]. Li^+ binding is retained on substitution of Gln^{32} and the residue-32 amide side chain appears critical in the liganding of Na^+ only [63]. The front-to-back packing would enable these residues to interact to form a cation binding site. As described in the structural model below, the packing also maximizes inter-subunit contact.

3. Structural organization and modeling of the c_{10} oligomer

Cross-linking experiments with native membranes provided evidence for the "front-to-back" packing of subunit *c* in a decameric ring with TMH-1 inside and TMH-2 outside [23,25,35]. The cross-links between genetically introduced cysteine residues were generated in part to test, and now do support, the NMR model [23]. High-yield dimers were formed with singly substituted Cys mutants from one face of TMH-1 only, which suggested an interior location for the helix in the ring structure, and a possible swiveling of subunits relative to each other during cross-linking. Several doubly Cys-substituted mutants formed extensive, multimeric ladders with the multimeric products extending to the range of c_{10}. Since multimeric products larger than dimers were formed, the initial cross-link leading to dimer formation must have been relatively nonperturbing to the structure. Due to ambiguities in estimating the number of cross-linked bands at the top of the gel, the maximal size of the multimers was not established with certainty in this study [23].

The number of *c* subunits in the F_o complex is at present the subject of controversy, with numbers in the range of 10–14 being proposed for different species [3,32–34]. We have most recently argued that the preferred number of *c* subunits in the oligomeric ring of *E. coli* is 10, based upon experiments where genetically fused trimers and tetramers were co-expressed and cross-linked into decameric structures [3]. Our most recent experiments were provoked by the report of Stock et al. [32] that a crystallized F_1–*c*-oligomer subcomplex from yeast mitochondria contained 10 *c* subunits. In very early isotopic labeling experiments with the *E. coli* enzyme, stoichiometries of 10 ± 1 subunit *c* were calculated for purified F_oF_1 [64], and 11–14 subunit *c* were estimated to be present per $(\alpha\beta)_3$ complex in crude membranes, where F_oF_1 had been genetically overproduced [64,65]. Subsequently, Jones and Fillingame [24] generated genetically fused dimers and trimers of *E. coli* subunit *c* that were functional, which by itself suggested that the final stoichiometry must be a multiple of two and three, and at that time, we considered the likely value to be 12. On introduction of Cys into the first and last helices of monomeric, dimeric and trimeric subunit *c*, disulfide cross-linking led to multimers, including in some cases a prominent c_{12} product, when visualized in the membrane by immunoblotting [24]. However, in subsequent experiments the oligomeric products of sizes $>c_{10}$ were shown to not copurify with the functional F_oF_1 complex, and the larger oligomers seen in the membrane concluded to be aberrant products of assembly [3]. In summary, the facile formation of c_{10} products from co-expressed, genetically fused trimers and tetramers indicates that the preferred stoichiometry of subunit *c* in *E. coli* F_oF_1 is 10, and is in accord with the stoichiometry seen in the mitochondrial F_1–c_{10} subcomplex reported by Stock et al. [32].

The studies reviewed above indicate that the *c* subunits in native F_o interact with the front face of one subunit packed against the back face of the next. The oligomer is packed such that the α-helical segments form two concentric rings with the N- and C-terminal helices located to the inner and outer ring respectively. The orientation of the *c* monomers with the N-terminal helices forming the inner ring provides the best fit to the cross-linking data of Jones et al. [23]. Further, the placement of helix-2 on the outside is strongly supported by the cross-linking experiments of Jiang and Fillingame [35], which show that multiple Cys in TMH-4 of subunit *a* can be cross-linked to multiple sites in TMH-2 of subunit *c*, whereas no cross-links from TMH-4 have been found to the multiple Cys introduced into TMH-1 of the subunit *c*.

The structure of the c_{10} oligomer has been modeled by molecular dynamics and energy minimization calculations from the solution structure of monomeric subunit *c* and 21 inter-subunit distance constraints derived from cross-linking of subunits in native F_1F_o [25]. The initial calculation was done for a c_{12} oligomeric ring [25], but the packing changes little when the structure is recalculated for the c_{10} oligomer [2] (Fig. 3). The subunits pack to form a compact hollow cylinder with an outer diameter of approximately 55 Å and an inner space with a minimal diameter of approximately 10 Å. A closure of the hole is obviously necessary to maintain the semi-permeable properties of the *E. coli* inner membrane, and we presume that it is filled with phospholipid as is the case of other ring-like structures, e.g. the *Rhodopseudomonas acidophilia* LH2 light harvesting complex [66] and the bacteriorhodopsin trimers in the purple membrane

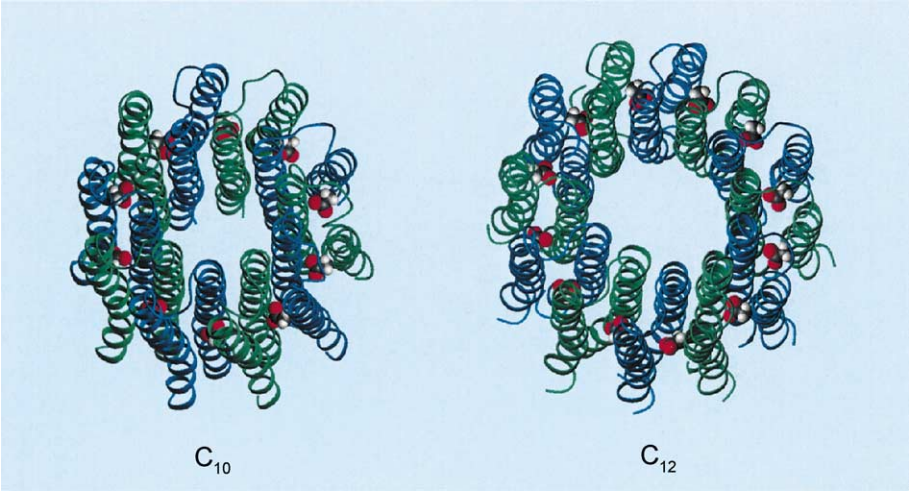

Fig. 3. Comparison of c_{10} and c_{12} oligomeric rings predicted using the cross-linking distance constraints of Dmitriev et al. [25]. The oligomeric cylinders are viewed from polar loop end of the subunit *c* hairpin. The Asp^{61} side chain of each subunit is shown.

of *Halobacterium salinarium* [67,68]. The TMHs pack in two concentric rings with TMH-1 on the inside and TMH-2 on the outside, as predicted by the cross-linking experiments. The H^+-transporting Asp^{61} residue packs towards the center of the four TMHs of two interacting subunit *c* in a position that is shielded from the lipid environment that is expected to surround the surface of the cylinder (Fig. 3). The packing supports the suggestion that the proton-binding site is formed at the packed interface of two subunits with Asp^{61} at the front face of one subunit interacting with Ala^{24}, Ile^{28} and Ala^{62} at the back face of a second subunit (Fig. 4). The positioning of these residues is minimally affected by the exact size of the *c*-ring, i.e. c_{10} versus c_{12} (Fig. 4). The positioning of the Asp^{61} carboxyl in the center of the interacting TMHs, rather than at the periphery of the cylinder, suggests that the helices may rotate or swivel to open the proton-binding site to subunit *a* during proton transport.

Rastogi and Girvin [52] have independently modeled the *c*-ring, using a similar set of cross-linking constraints as in Dmitriev et al. [25] and somewhat different molecular dynamics and simulated annealing approaches. The major difference in approach was greater stringency in imposition of NMR constraints from the monomeric model. These additional constraints resulted in less reorganization in the structure of individual helices during the packing of subunit monomers into a ring, and a slightly less compact final structure.

4. Modeling *c*-ring interactions with subunits ε and γ

The polar loop of subunit *c* was proven to interact directly with the γ and ε subunits of F_1 by Cys–Cys cross-linking experiments[26,27], the initial experiments being provoked by a suppressor mutation analysis that indicated that conserved cQ42 interacted with εE31 [54]. In a subsequent, more extensive analysis [28], cross-link formation was interpreted by use of the solution NMR structures of subunits *c* and ε [22,29]. Cysteine introduced into the continuous span of residues ε26–33 was shown to cross-link to Cys at positions 40, 42 and 44 in loop of subunit *c*. Residues 26–33 of subunit ε form a turn of antiparallel β-sheet extending from the bottom of the ε subunit as a well-defined lobe (Fig. 5). The side chains of residues 42 and 44 project from opposite sides of the loop of subunit *c*, i.e. the "front" and "back" face, respectively, which indicates that the cross-linkable domain of ε must pack between the loops of adjacent subunit *c* in the c_{10} ring. The interaction of subunits has been modeled by molecular dynamics and energy minimization, based upon cross-linking distance constraints, and places the residue 26–33 lobe of subunit ε between loops of subunit *c* in a well-packed structure (Fig. 5). The modeling indicates that the cross-linking of subunit γ with these same residues in subunit *c* [27] must take place by interaction with a separate pair of *c* subunits, perhaps the adjacent pair, in the oligomer.

5. Other models for subunit *c* and the oligomeric *c*-ring

An alternate model for the structure of *P. Modestum* subunit *c* as it folds in the lipid bilayer has been proposed by Dimroth et al. [69,70], based upon the secondary structure observed in sodium dodecyl sulfate (SDS) micelles by NMR [71]. A prominent break in the α-helical structure of TMH-1 was observed around Pro^{28}, which corresponds to *E. coli* residue 24, and a break in the α-helical structure of TMH-2 also observed around the Glu^{65}–Ser^{66} cation binding site [71]. However, the NMR evidence fell short in providing information on interactions between segments of secondary structure and whether the protein actually folded back on itself. Based upon other nonstructural evidence, a model for insertion of

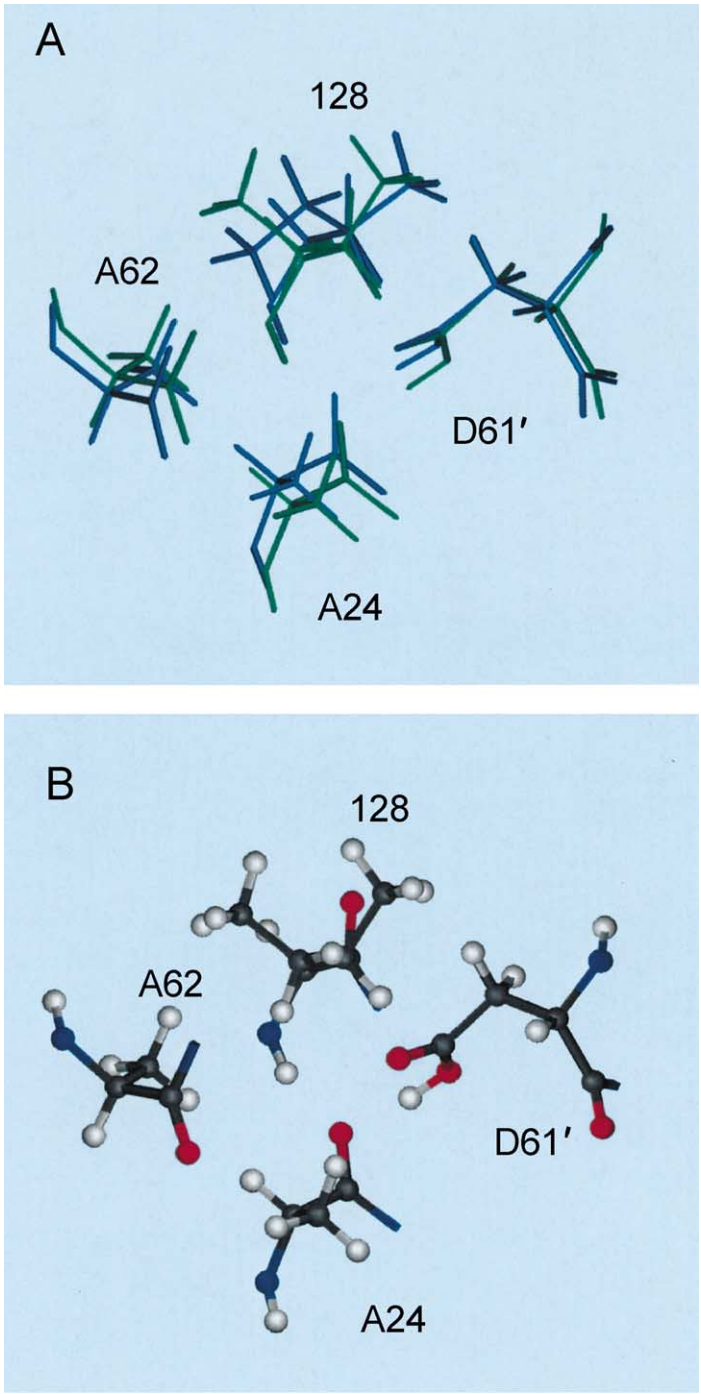

Fig. 4. Comparison of the relative positions of Asp[61] side chain at the "front" face of one subunit *c* to the Ala[24], Ile[28] and Ala[62] side chains at the "back" face of an interacting subunit *c* in c_{10} and c_{12} oligomeric rings. (A) Overlay of interacting subunits in c_{10} (green) and c_{12} (blue) oligomeric ring. (B) Positions of the interacting residues in the c_{10} ring.

the protein in a lipid bilayer was proposed in which the Gln[32], Glu[65] and Ser[66] cation binding residues were placed near the cytoplasmic (F_1-binding) surface of the membrane [69,70]. The N- and C- terminal α-helices were presumed to extend to the periplasmic surface of the membrane, despite their short length, and residues 33–64 suggested to form a long, helical hairpin loop extending into the cytoplasm.

An alternative model for the *c* oligomer in which TMH-2 is packed in the inner ring and TMH-1 in the outer ring was proposed by Groth and Walker [72]. Intuitively, the model seems less likely since the cross-sectional diameter of TMH-2 is considerably greater than that of TMH-1 and the packing the TMH-1 on the inside is supported by the aforementioned cross-linking experiments and energy calculations [25,52]. In attempts to probe and distinguish the

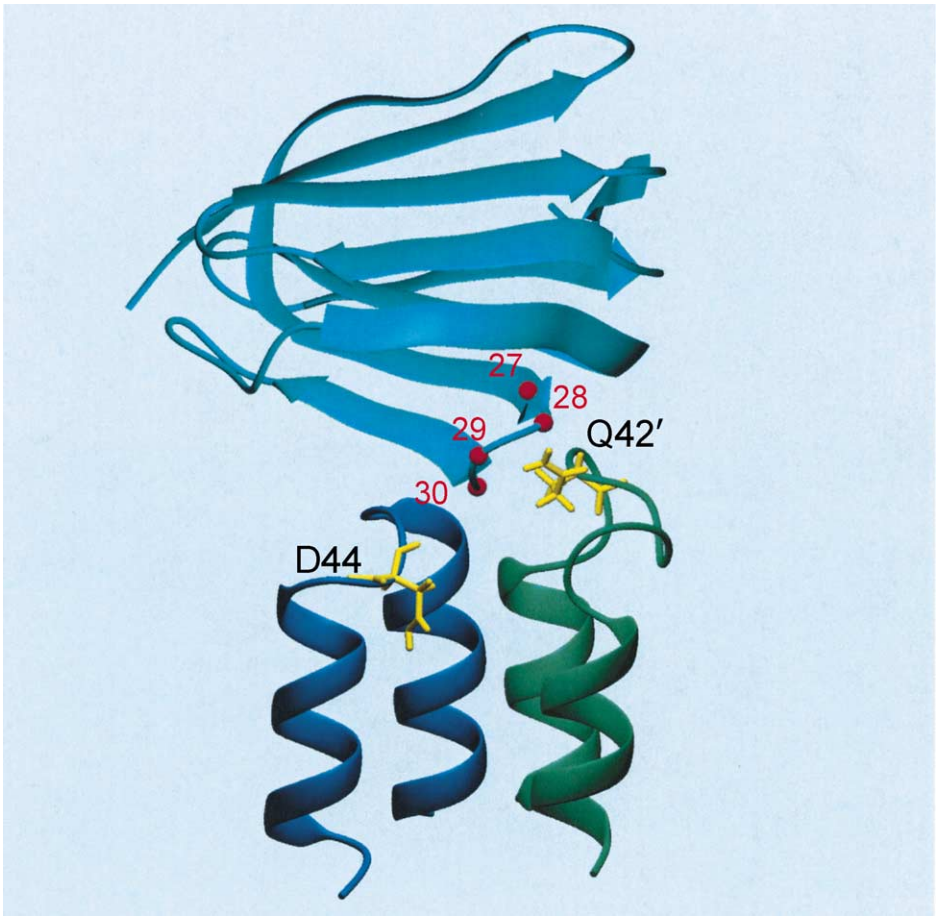

Fig. 5. Model for binding of β-sandwich domain of subunit ε between polar loops of the *c*-ring [28]. Model is based upon cross-linking of the *c* and ε subunits via residues discussed in text, and the NMR structures of the subunits. Residue Gln^{42} is shown projecting from the "front" face of subunit *c*′ and residue Asp^{44} is shown projecting from the "back" face of a different subunit *c*. The loop of subunit ε including residues 26–33 can be cross-linked to either $cGln^{42}$ or $cAsp^{44}$.

arrangement of subunits, Groth and coworkers introduced single Trp substitutions in residues 12–24 of TMH-1 and residues 61–72 of TMH-2 [73,74]. The Trp scanning mutagenesis strategy is based upon the assumption that a bulky Trp side chain in an area of close protein–protein contact will disrupt function due to steric conflicts with neighboring residues. Conversely, a Trp side chain at the surface of the ring would be easier to accomodate without disruptive effects on activity. Based upon their analysis of steric clashes, Groth et al. [73,74] concluded that a ring structure with TMH-2 on the inside was somewhat more likely, although the alternative arrangement with TMH-1 on the inside was also considered plausible [74]. A variation of the *TMH-2-inside* model was also considered in which the packing of subunits is staggered with every other monomer displaced more towards the inside or outside of the ring [73].

We have argued that interpretation of the effects of most of the substitutions, where activities were severely compromised or nil, is complicated and probably not strong evidence for either model. Some activity was observed with substitutions centered around Pro^{64}, i.e. at residues 62, 63 and 65, which may reflect a requirement for structural flexibility in this region (see Section 8). The differing effects of substitutions at positions 69–72 are quite consistent with an α-helical periodicity and the model presented by Dmitriev et al. [25], the expected positions of these side chains having been discussed more thoroughly in that reference . In addition, the Groth and Walker [72] model is not easily reconciled with the extensive pattern of cross-linking observed between cysteine residues in TMH-2 of subunit *c* and cysteine residues in TMH-4 of subunit *a*, as was discussed above.

We have quantitatively tested the structural/energetic effects of these Trp substitutions in our model for the *c* oligomer. Trp-substituted *c*-oligomers were energy minimized as in Dmitriev et al. [25], and the difference in potential energy between the mutant and wild-type structures used as a measure of the disruptive effect of the mutation. Calculations were carried out on both c_{10} and c_{12} substituted oligomers and the differences in potential energies did not differ appreciably. We present the data for the c_{10} oligomer here and have compared it to the steric conflict values calculated by Groth and coworkers [73,74].

In the initial paper on TMH-2 substitutions, Groth et al. [73] used a c_{12} oligomeric model, and in the second paper on TMH-1 substitutions, compared steric conflict values in c_9, c_{10} and c_{12} oligomers [74]. Again, the exact number of *c* subunits in the ring seemed to result in only marginal differences in the extent of steric conflict. In Fig. 6, we relate the effect of each Trp substitution on ATPase coupled proton pumping activity to the calculated steric conflict in the *TMH-2-inside* model (Panel A) and to the difference in potential energy in the *TMH-1-inside* model (Panel B). Both models correctly predict a non-functional phenotype for several severely disruptive mutants.

When the data sets for the two TMHs are analyzed separately, important differences emerge. For TMH-1, four of eight mutants showing $\leq 6\%$ proton pumping activity give negative steric conflict values in the *TMH-2-inside* model, indicating no steric clash, whereas all eight mutants show large positive differences in potential energy (disruptive structural effects) in the *TMH-1-inside* model. Further, the data from the *TMH-1-inside* model fit a smoother, more monotonic function in relating the potential energy changes in the structure to activity. The notable exception is the A17W, a mutation which shows 50% activity despite a potential energy that is predicted to be disruptive. The general fit of the curve is consistent with a simple model where the oligomeric structure breaks down and activity falls to zero once the energy penalty for incorporating the substitution exceeds the stability threshold. In our *TMH-1-inside* model, the N-terminal helix is isolated from the bulk lipid and does not contact other F_o subunits, and its conformation is not predicted to change significantly during the catalytic cycle. The effect of Trp substitutions on activity is therefore expected to be predicted well from the potential energy of the *c*-oligomeric structure alone.

The situation is more complicated for TMH-2 since it is predicted to be in contact with other F_o subunits in the *TMH-1-inside* model; the helix is also predicted to rotate during the catalytic cycle. Almost all of the substitutions in TMH-2 cause major decreases in activity. For these substitutions, the calculated steric conflicts in the *TMH-2-inside* model are a better predictors of activity than were the substitutions in TMH-1. The notable exception is the A67W mutant that shows no activity but a negative steric conflict value. For the *TMH-1-inside* model, most mutations are also predicted to be disruptive by the potential energy calculations, but correlation between activity and potential energy is less pronounced. Several mutants with rather small changes in potential energy show loss of function, which

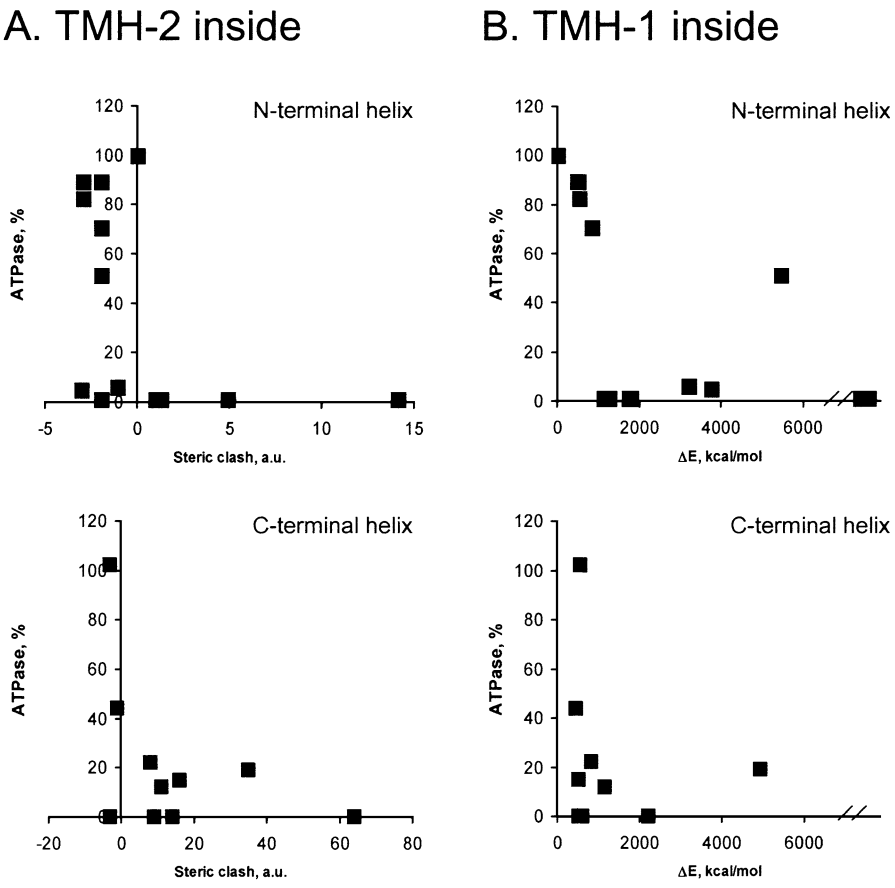

Fig. 6. Relationship of residual activity in Trp substituted mutants of subunit *c* to steric clash (A) potential energy differences (B) calculated from *TMH-2-inside* and *TMH-1-inside* models for *c*-ring. (A) ATPase-coupled H^+ pumping activity and steric clash values calculated for *TMH-2-inside* models [73,74]. Note the difference in scales for the N- versus C- terminal helices. (B) Differences in potential energy calculated for the same set of mutants using *TMH-1-inside* model.

may reflect the necessity of movement/rotation of TMH-2 during the catalytic cycle, or the necessity of close packing with subunit *a*. In our model, the Ala^{67} side chain is positioned at the periphery of the ring, and the complete loss of function in the A67W mutant is easily understood if the helix rotates as is discussed in greater detail below. In summary, the Trp substitutions generated by Groth and coworkers do not clearly distinguish between the TMH-1 inside or outside models by their own analysis [74], and by the energy calculations discussed here fit better with the *TMH-1-inside* model.

Stock et al. [32] have noted the obvious correlation between the electron density of the *c*-oligomer in a crystallized F_1-c_{10} subcomplex from yeast mitochondria and the NMR structure and oligomeric model of *E. coli* subunit *c*. Although the exact position of individual side chains is uncertain in the 3.9-Å resolution structure, the extended α-helices and hairpin turn seen in the NMR model of *E. coli* subunit *c* closely fit the published electron density map. As in the *E. coli* oligomeric model, the shorter somewhat kinked TMH-2 was concluded to pack at the outer circumference of the oligomeric ring. In addition, the long, extended α-helices seen in the Stock et al. structure argue against the suggested folding of *P. modestum* subunit *c* [69,70], i.e. the model based upon the NMR-determined secondary structure in SDS micelles [71]. Stock et al. [32] also modeled the backbone structure of *E. coli* subunit ε into the density map. The two domains of the *E. coli* ε subunit, previously determined by both NMR and X-ray crystallography [29,30], were easily recognized. The antiparallel loop of β sheet that had previously been shown to cross-link with the polar loop of subunit *c* [28] was proposed to lie at the F_1-c_{10} interface. The specifics of docking of the ε subunit with the *c*-ring differs somewhat in the model of Hermolin et al. [28], and in the docking suggested by the coordinates deposited by Stock et al. (1qo1; Ref. [32]). A more recent proposal for the docking of the two structures [31], based upon the crystal structure of an *E. coli* γε subcomplex, is more in accord with the Hermolin et al. model and the cross-linking data.

6. Changes in *c* subunit structure with deprotonation of aspartyl-61

Rastogi and Girvin [52] solved the structure of subunit *c* at pH 8 in the same chloroform–methanol–water solvent mixture used to solve the initial structure at pH 5. Asp^{61} has a pK_a of 7.1 in this solvent system with the pK_a's of all other carboxyl groups falling below 6 [61]. Thus, Asp^{61} should be fully protonated at pH 5 and nearly completely deprotonated at pH 8. Major structural changes in the loop region of the protein were known to take place over the pH range in which Asp^{61} ionized [61], and those changes were described in detail in the Rastogi and Girvin [52] pH 8 structure. The key change was a rearrangement in the packing of transmembrane helices such that TMH-2 was rotated by 140° with respect to TMH-1 with a consequent displacement of the Asp^{61} side chain from the "front" to the "back" surface. The structure of segments of helical backbone differed little between the pH 5 and pH 8 structures when viewed individually, and the major change was a reorientation of helices due to a twisting in the C-terminal region of the polar loop between Pro^{43} and Thr^{51} (Fig. 7A versus B). The new structure was modeled into a ring of otherwise protonated *c* subunits, and a novel hypothesis for how a protonation/deprotonation-triggered turning of TMH-2 could drive a stepwise rotation of the ring relative to $a\text{Arg}^{210}$ in the peripheral stator was proposed. Central to the model is the predicted packing of $a\text{Arg}^{210}$ between a deprotonated Asp^{61} side chain at the back face of one subunit *c* (folded as in the pH 8 structure) and a protonated Asp^{61} side chain at the front face of next subunit *c* (folded as in the pH 5 structure). Protonation of the ionized Asp^{61} was predicted to cause a rotation of TMH-2 and a repacking of the side chain in its expected protonated position at the original front face of the molecule. The rotation of TMH-2 back to its original position was predicted to be coupled with the movement of the Arg^{210} residue between a new set of fully protonated subunits, the movement in turn driving the stepwise ratcheting of the rotor. Subsequent deprotonation of the next subunit would trigger rotation of the ionized Asp^{61} side chain to the back face of the subunit to generate the equivalent of the pH 8 structure, and again placing the Arg^{210} side chain between the ionized and protonated Asp^{61} side chains, i.e. as in the starting position.

The pH 8 structure of Rastogi and Girvin [52] raises several major questions that have yet to be resolved. The first regards interpretation of the structural changes observed in solution since it could be argued that such structural changes might be muted by other subunit–subunit protein contacts. In support of the model presented, Rastogi and Girvin [52] have argued that the *a*–*c* cross-linking results of Jiang and Fillingame [35] support a model in which TMH-2 of the pH 5 structure is rotated as in the pH 8 structure. Residues 62, 65 and 69, which form high yield cross-links with subunit *a*, lie at the packing interface between helices of the monomer in the case of Gly^{69}, or at the packing interface between subunits for Ala^{62} and Met^{65}. The reorientation of TMH-2 or insertion of *a*TMH-4 between subunits of the oligomer during proton translocating function has also been suggested by Jiang and Fillingame [35] and Fillingame et al. [37]. Rationalizing major structural changes in the loop regions of subunits of the oligomeric rotor is more difficult. The c_{10}-oligomer has been shown to rotate as a unit with the γε complex of F_1, and indeed cross-linking of γε–*c* into heterotrimers was shown to have negligible effects on function [15,75]. A permanent association of γε with a given set of *c*-subunits of the oligomer is apparently possible in a functional complex. The large conformational changes in the loop region, as implied by comparing the NMR structures at pH 5 and pH 8, would be

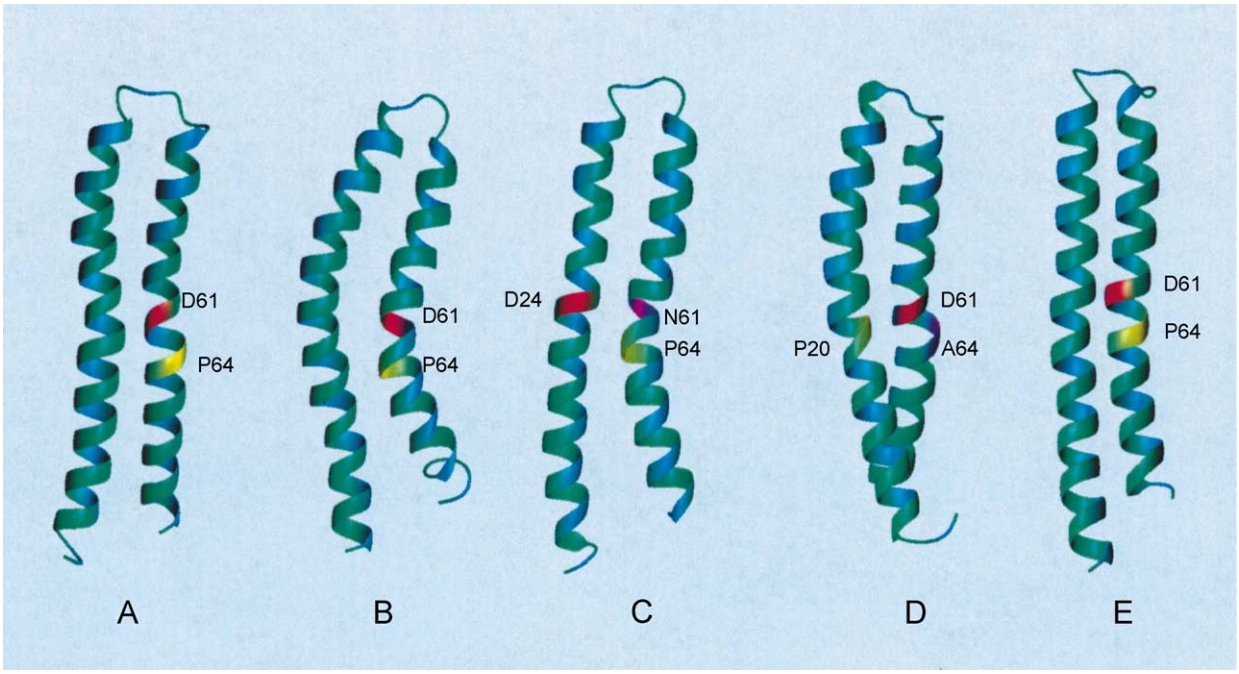

Fig. 7. Ribbon diagram comparing the structures of wild-type and mutant subunit *c*. (A) Wild-type subunit *c* at pH 5 (1c0v [52]). (B) Wild-type subunit *c* structure at pH 8 (1c99 [52]). (C) D24N61 subunit *c* at pH 5 (1L6T [76]). (D) P20A64 subunit *c* at pH 5 (1IJP [59]). (E) Subunit *c* monomer from the model of *c*-ring (1J7F [25]).

expected to disrupt the $\gamma\varepsilon-c$ interactions. Perhaps these changes are suppressed in the $c_{10}-\gamma\varepsilon$ complex, although clearly conformational changes near the loop region would be required for the postulated helical rotation.

Finally, the models discussed by Rastogi and Girvin [52] and Fillingame et al. [37], where TMH-2 is postulated to turn to bring *c*Asp^{61} in proximity to *a*Arg^{210}, fall short in explaining the function of the functional aspartate interchange mutants in which the proton-transporting carboxyl is switched from residue 61 in TMH-2 to residue 24 in TMH-1. The turning of *c*TMH-2 would not be expected to change the proximity of the Asp^{24} side chain to *a*Arg^{210}. One might dismiss rationalization of function in the Asp^{24} interchange mutants as being unimportant because of the rather feeble function of the original Asp^{24}Gly^{61} mutant [55], but some Asp^{24} mutants with secondary, optimizing mutations in subunit *a* grow as well as wild type via oxidative phosphorylation [51]. The NMR structure of the Asp^{24}Asn^{61} variant of subunit *c* discussed below has provided hints of a possible explanation.

7. Structure of the D24N61 aspartate interchange mutant

As originally shown by Miller et al. [55] with the D24G61double mutant, the essential aspartyl residue of subunit *c* can be moved from position 61 in TMH-2 to position 24 in TMH-1 with retention of significant function. Subsequently, greater function was shown with the D24N61 substituted protein [56], and hence this protein was used for NMR structural studies at pH 5 where Asp^{24} was shown to be protonated (pK_a = 6.9; Ref. [61]). Surprisingly, the structure strongly resembles the structure of wild-type subunit *c* at pH 8, where Asp^{61} is deprotonated and *c*TMH-2 rotated relative to the structure at pH 5 (Ref. [76] and Fig. 7C). The solution structures of the polar loops of the wild-type protein at pH 8 and the D24N61 protein at pH 5 also bear a close resemblance. The results suggest that the essential aspartate, whether at position 61 or position 24, may gain accessibility to *a*R210 by a swiveling of helices within a single *c* subunit to shift the position of the carboxyl from the front to the back of the molecule, and that the swiveling occurs in concert with rotation of *c*TMH-2. Based upon this structure, we have suggested that there are two general stable conformational isomers of subunit *c* that vary in the orientation by which *c*TMH-2 is packed with *c*TMH-1. Further, we propose that the switch in helical orientation is not dictated by the ionization state of the essential aspartate group, since Asp^{24} is protonated in the NMR solution structure of the D24N61 mutant. This has led to an adaptation of the model of Rastogi and Girvin [52], as is discussed below.

The adaption of the Rastogi and Girvin model is depicted in Fig. 8A. One of the subunits of the oligomeric ring (the *n*th) is shown as in the pH 8 structure with TMH-2 rotated with respect to the other subunits. The key differences are that we predict that helical rotation occurs before the ionization of Asp^{61}, and that the helical movement to the position shown takes place via a clockwise rotation of

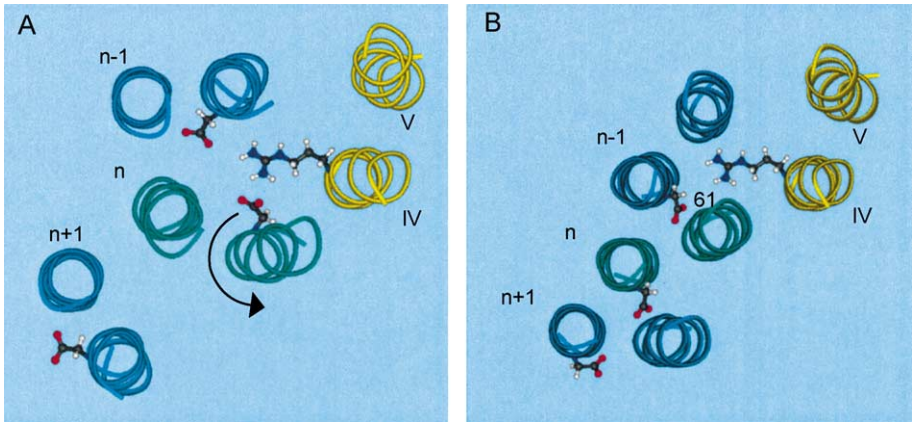

Fig. 8. Possible adaptation of the rotational model of Rastogi and Girvin [52] to the function of D24N61 substituted subunit *c*. (A) Adaptation of model proposed by Rastogi and Girvin for wild-type *c*-oligomer. In the model, a single subunit *c* with Asp^{61} ionized (the *n*th subunit) is placed in a ring of otherwise protonated subunit *c*. TMH-2 of the ionized subunit *c* is rotated relative to the TMH-2 of other subunits and the position of the Asp^{61} side chain is displaced from one side to the other as in the pH 8 structure. The proposed interaction of ionized Asp^{61} with $aArg^{210}$ is indicated. The hypothetical TMH-4 and TMH-5 of subunit *a* are indicated by Roman numerals IV and V. The helical rotation indicated by the arrow is discussed in the text. (B) Adaptation of the Rastogi and Girvin mechanistic model to the modeled ring structure of D24N61 subunit *c*. The position of Asn^{61} in subunit *n* is indicated by the residue number.

TMH-2. The helical rotation leading to this state is then postulated to expose $cAsp^{61}$ to Arg^{210} in *a*TMH-4. Asp^{61} subsequently deprotonates in the new environment due to its proximity to *a*R210. This sequence would fit best with the structure of the D24N61 protein, described here, where TMH-2 is turned and Asp^{24} still protonated. Following deprotonation of Asp^{61}, helical interactions elsewhere in the putative proton channels of subunit *a*, which would be driven by the force of the proton gradient, would cause $aArg^{210}$ to move away from the Asp^{61} carboxylate group to enable reprotonation of the ionized carboxylate from the periplasmic inlet channel. The reprotonated *c*TMH-2 would then rotate back to its original position with respect to *c*TMH-1 by swiveling in the counterclockwise direction, as shown by the arrow in Fig. 8A. This helical rotation would be coupled to the counterclockwise movement of the oligomeric ring, i.e. movement of subunit *n* to the position occupied by subunit $(n-1)$, etc., with the simultaneous swiveling of $cTMH\text{-}2_{(n+1)}$ and insertion of *a*R210 between subunits $(n+1)$ and *n*. The latter could occur if the helices of subunits *a* and *c* rotated around each other in a manner akin to meshed gears.

Application of the model to the D24N61 mutant is considered in Fig. 8B. In this case, all subunits are shown as resolved in the single D24N61 NMR structure, although helical rotations to alternate conformations might be predicted by application of the model considered above in a more complicated scenario. The placement of subunits in the modified ring is based upon a best fit of paired helical segments from the D24N61 NMR structure to equivalent helices in the wild-type *c*-ring [76]. The structure of D24N61 subunit at position *n* resembles wild-type subunit *n* (Fig. 8A) with Asn^{61} in TMH-2 positioned proximally to *a*R210, i.e. at the same position of Asp^{61} in wild type at pH 8. The insertion of *a*R210 between subunits *n* and $(n-1)$ would in this case lead to the deprotonation of Asp^{24} of subunit $(n-1)$. Following movement of *a*R210 to facilitate reprotonation of $Asp^{24}{}_{(n-1)}$, TMH-2 of subunit *n* would swivel in the counterclockwise direction to facilitate movement of the rotor as in the case of the wild-type rotor. The model described above leaves open the question of whether TMH-1 also swivels in a concerted fashion during the rotations of TMH-2. Movement of the essential carboxyl from one face of *c* monomer to the other may be a necessary feature of the ion-binding and release interactions at the *a*–*c* interface. A concerted swiveling of both helices would provide a general mechanism applicable to both proteins.

In summary, the NMR structure of D24N61 subunit *c* leads to a revised view of how conformational changes linked to protonation/deprotonation of subunit *c* may drive movement of the *c* rotor via a concerted swiveling of helices driven by the protonmotive force. The structure leads to the prediction that *c*TMH-2 swivels before the aspartate is deprotonated, and that this movement is prerequisite to $aArg^{210}$ subsequently lowering the pK_a of the essential carboxyl group. The movements obviously have to be coupled to the opening and closing of outlet and inlet channels in the still unresolved structure of subunit *a*.

8. Role of transmembrane proline as suggested by the structure of a helix-2/helix-1 prolinyl interchange mutant

One prominent feature of the wild-type subunit *c* structure is a bend in TMH-2 associated with Pro^{64} (Figs. 2 and 7A). Substitution of Pro^{64} with Leu or Ala renders the ATP synthase inactive, but interestingly, function in the Pro^{64} mutants is restored by the A20P second site mutation [58,59]. Perhaps, surprisingly, the P20A64 mutant grows as well as wild type and the F_oF_1 complex is fully functional in ATPase coupled H^+ pumping [59]. Residues 20 and 64 lie

directly opposite of each other in the hairpin structure of subunit *c* (Fig. 2). The structure of the P20A64 *c* subunit was determined at pH 5 with the same solvent system used with the wild-type protein. As in the case of the wild-type protein, P20A64 subunit *c* forms a hairpin of two α-helices, with residues 41–45 forming a connecting loop, but in this case, Pro^{20} induces a bend in TMH-1 which then packs against a more straightened TMH-2 (Fig. 7D). The helices cross at angles of about 20° for the segments comprising residues 22–40 and 46–62 and about 35° for the segments comprising residues 4–18 and 64–77. The changes in orientation and crossing angle of the helices in the mutant versus wild-type proteins result in associated changes in structure of the connecting polar loop, most notably of residues 42–45 [59].

From the structure of P20A64 subunit *c* described above, we conclude that the essential prolinyl residue will tend to introduce a bend into the TMH in which it is placed, when the helical hairpin is formed within a subunit monomer. Since the prolinyl residue and associated bend occur in different TMHs in the wild-type and mutant proteins, the packing of TMHs varies somewhat in the structures of the two monomeric subunits. On the other hand, the function of the P20A64 mutant ATP synthase is indistinguishable from wild-type, which strongly suggests that the structure of both proteins should be very similar within the oligomeric *c*-ring. We suggest that intersubunit packing interactions leading to *c*-ring formation are likely to force an adjustment (straightening) in either structure. In contrast to globular proteins, there are relatively few surface–surface interactions between the TMHs of the highly elongated subunit *c* monomer. The relative orientation and bend of helices should therefore be expected to change significantly upon packing of the individual *c* subunits into the ring structure due to the contribution of the numerous additional interactions [25,52]. Indeed, the modeling of the wild-type *c* oligomer indicated that the C-terminal helix straightened with the bend angle around Pro^{64} being reduced from 27° in the NMR structure (1A91, Ref. [22]) to 16 ± 3° in the oligomer ring ([25]; Fig. 7E). Further, a more recent calculation of the wild-type subunit *c* structure at pH 5 (1C0V [52]) showed a less pronounced bend around Pro^{64} of about 11°. Given that the two pH 5 structures do differ significantly and that the calculations were based upon the same extensive set of NOEs [22], the experimentally derived constraints clearly permit significant variation in the overall bend of the molecule. In the case of P20A64 subunit *c*, a straightening of helix-1 and concomitant reorientation of the two helical segments in the course of oligomer formation may allow the subunit to pack in a ring which is very similar to wild type. The structure presented here does indicate that the forces leading to the kink in TMH-2 of wild-type subunit *c* result from local constraints introduced by the prolinyl residue rather than global interactions reflecting the packing of the entire protein. The helix-breaking kink observed in TMH-1 of the *P. modestum* subunit *c*, as determined in SDS micelles ([71]; see Section 5), may arise from similar local constraints.

The comparison of the structures of wild-type and P20A64 subunit *c* raises an obvious question about the functional role of the bend in the proline-containing helix. The structure of deprotonated subunit *c* at pH 8 provided the first structural evidence for a major reorientation of helices during the catalytic cycle. Helical turning within the confines of the multiple intersubunit surface contacts would require rather complex concerted movements of both TMHs and would likely also involve the neighboring *c* subunits. The movement appears to involve changes in the bend angle of both helices. Indeed, in the pH 8 structure of the wild-type monomeric subunit, very significant bends are observed in both TMH-2 and TMH-1 (Fig. 7B). The fact that the proline can be located on either of the two helices without a noticeable effect on function supports the notion that both helices are involved. The role of prolinyl residue would then be to introduce a "weak spot" in the helical hairpin by breaking the regular pattern of hydrogen bonds stabilizing one of the TMHs. A comparison of the sequences of subunit *c* from different species indicates the presence of a prolinyl residue in close proximity to the residue homologue of *E. coli* Asp^{61} in 75% of the species, with the proline placed in TMH-1 or TMH-2 with nearly equal probability [60]. In the species lacking a proline, with one exception, Ser or Thr residues are found in these regions on one or both helices. Hydrogen bond formation between a Ser or Thr side chain and the backbone atom of another residue provides an alternative mechanism of breaking the hydrogen bond pattern of an α-helix and introducing a potential site for the swiveling and bending of the helix. In summary, the bends observed in the TMHs of wild-type and P20A64 subunit *c* in solution very likely reflect upon a need for a concerted structural rearrangement of helices around the region of the essential proline during the H^+ transport cycle.

References

[1] A.E. Senior, Physiol. Rev. 68 (1988) 177–231.
[2] R.H. Fillingame, W. Jiang, O.Y. Dmitriev, J. Bioenerg. Biomembranes 32 (2000) 433–439.
[3] W. Jiang, J. Hermolin, R.H. Fillingame, Proc. Natl. Acad. Sci. U. S. A. 98 (2001) 4966–4971.
[4] J.P. Abrahams, A.G.W. Leslie, R. Lutter, J.E. Walker, Nature 370 (1994) 621–628.
[5] C. Gibbons, M.G. Montgomery, A.G.W. Leslie, J.E. Walker, Nat. Struct. Biol. 7 (2000) 1055–1061.
[6] T.M. Duncan, V.V. Bulygin, Y. Zhou, M.L. Hutcheon, R.L. Cross, Proc. Natl. Acad. Sci. U. S. A. 92 (1995) 10964–10968.
[7] D. Sabbert, S. Engelbrecht, W. Junge, Nature 381 (1996) 623–625.
[8] H. Noji, R. Yasuda, M. Yoshida, K. Kinosita Jr., Nature 386 (1997) 299–302.
[9] J. Weber, A.E. Senior, Biochim. Biophys. Acta 1458 (2000) 300–309.
[10] C. Tang, R.A. Capaldi, J. Biol. Chem. 271 (1996) 3018–3024.
[11] Y. Kato-Yamada, H. Noji, R. Yasuda, K. Kinosita Jr., M. Yoshida, J. Biol. Chem. 273 (1998) 19375–19377.

[12] Y. Sambongi, Y. Iko, M. Tanabe, H. Omote, A. Iwamoto-Kihara, I. Ueda, T. Yanagida, Y. Wada, M. Futai, Science 286 (1999) 1722–1724.
[13] O. Pänke, K. Gumbiowski, W. Junge, S. Engelbrecht, FEBS Lett. 472 (2000) 34–38.
[14] M. Tanabe, K. Nishio, Y. Iko, Y. Sambongi, A. Iwamoto-Kihara, Y. Wada, M. Futai, J. Biol. Chem. 276 (2001) 15269–15274.
[15] S.P. Tsunoda, R. Aggeler, M. Yoshida, R.A. Capaldi, Proc. Natl. Acad. Sci. U. S. A. 98 (2001) 898–902.
[16] S.B. Vik, B.J. Antonio, J. Biol. Chem. 269 (1994) 30364–30369.
[17] S. Engelbrecht, W. Junge, FEBS Lett. 414 (1997) 485–491.
[18] T. Elston, H. Wang, G. Oster, Nature 391 (1998) 510–513.
[19] R. Birkenhäger, M. Hoppert, G. Deckers-Hebestreit, F. Mayer, K. Altendorf, Eur. J. Biochem. 230 (1995) 58–67.
[20] K. Takeyasu, H. Omote, S. Nettikadan, F. Tokumasu, A. Iwamoto-Kihara, M. Futai, FEBS Lett. 392 (1996) 110–113.
[21] S. Singh, P. Turina, C.J. Bustamante, D.J. Keller, R.A. Capaldi, FEBS Lett. 397 (1996) 30–34.
[22] M.E. Girvin, V.K. Rastogi, F. Abildgaard, J.L. Markley, R.H. Fillingame, Biochemistry 37 (1998) 8817–8824.
[23] P.C. Jones, W. Jiang, R.H. Fillingame, J. Biol. Chem. 273 (1998) 17178–17185.
[24] P.C. Jones, R.H. Fillingame, J. Biol. Chem. 273 (1998) 29701–29705.
[25] O.Y. Dmitriev, P.C. Jones, R.H. Fillingame, Proc. Natl. Acac. Sci. U. S. A. 96 (1999) 7785–7790.
[26] Y. Zhang, R.H. Fillingame, J. Biol. Chem. 270 (1995) 24609–24614.
[27] S.D. Watts, C. Teng, R.A. Capaldi, J. Biol. Chem. 271 (1996) 28314–28347.
[28] J. Hermolin, O.Y. Dmitriev, Y. Zhang, R.H. Fillingame, J. Biol. Chem. 274 (1999) 17011–17016.
[29] S. Wilkens, F.W. Dahlquist, L.P. McIntosh, L.W. Donaldson, R.A. Capaldi, Nat. Struct. Biol. 2 (1995) 961–967.
[30] U. Uhlin, G.B. Cox, J.M. Guss, Structure 5 (1997) 1219–1230.
[31] A.J.W. Rodgers, M.C.J. Wilce, Nat. Struct. Biol. 7 (2000) 1051–1054.
[32] D. Stock, A.G.W. Leslie, J.E. Walker, Science 286 (1999) 1700–1705.
[33] H. Seelert, A. Poetsch, N.A. Dencher, A. Engel, H. Stahlberg, D.J. Müller, Nature 405 (2000) 418–419.
[34] H. Stahlberg, D.J. Müller, K. Suda, D. Fotiadis, A. Engel, T. Meier, U. Matthey, P. Dimroth, EMBO Rep. 2 (2001) 229–233.
[35] W. Jiang, R.H. Fillingame, Proc. Natl. Acad. Sci. U. S. A. 95 (1998) 6607–6612.
[36] O. Dmitriev, P.C. Jones, W. Jiang, R.H. Fillingame, J. Biol. Chem. 274 (1999) 15598–15604.
[37] R.H. Fillingame, W. Jiang, O.Y. Dmitriev, J. Exp. Biol. 203 (2000) 9–17.
[38] S.D. Dunn, D.T. McLachlin, M. Revington, Biochim. Biophys. Acta 1458 (2000) 356–363.
[39] R.A. Capaldi, B. Schulenberg, J. Murray, R. Aggeler, J. Exp. Biol. 203 (2000) 29–33.
[40] K. Altendorf, W.-D. Stalz, J.-C. Greie, G. Deckers-Hebestreit, J. Exp. Biol. 203 (2000) 19–28.
[41] S. Wilkens, R.A. Capaldi, Nature 393 (1998) 29.
[42] B. Böttcher, L. Schwarz, P. Gräber, J. Mol. Biol. 281 (1998) 757–762.
[43] J.E. Walker, Angew. Chem., Int. Ed. Engl. 37 (1998) 2308–2319.
[44] S.D. Dunn, J. Chandler, J. Biol. Chem. 273 (1998) 8646–8651.
[45] A.J.W. Rodgers, R.A. Capaldi, J. Biol. Chem. 273 (1998) 29406–29410.
[46] D.T. McLachlin, S.D. Dunn, Biochemistry 39 (2000) 3486–3490.
[47] P.J. Jones, J. Hermolin, W. Jiang, R.H. Fillingame, J. Biol. Chem. 275 (2000) 31340–31346.
[48] F.I. Valiyaveetil, R.H. Fillingame, J. Biol. Chem. 273 (1998) 16241–16247.
[49] J.C. Long, S. Wang, S.B. Vik, J. Biol. Chem. 273 (1998) 16235–16240.
[50] T. Wada, J.C. Long, D. Zhang, S.B. Vik, J. Biol. Chem. 274 (1999) 17353–17357.
[51] D. Fraga, J. Hermolin, R.H. Fillingame, J. Biol. Chem. 269 (1994) 2562–2567.
[52] V.K. Rastogi, M.E. Girvin, Nature 402 (1999) 263–268.
[53] D. Fraga, J. Hermolin, M. Oldenburg, M. Miller, R.H. Fillingame, J. Biol. Chem. 269 (1994) 7532–7537.
[54] Y. Zhang, M. Oldenburg, R.H. Fillingame, J. Biol. Chem. 269 (1994) 10221–10224.
[55] M.J. Miller, M. Oldenburg, R.H. Fillingame, Proc. Natl. Acad. Sci. U. S. A. 87 (1990) 4900–4904.
[56] Y. Zhang, R.H. Fillingame, J. Biol. Chem. 269 (1994) 5473–5479.
[57] R.H. Fillingame, M. Oldenburg, D. Fraga, J. Biol. Chem. 266 (1991) 20934–20939.
[58] A.L. Fimmel, D.A. Jans, L. Langman, L.B. James, G.R. Ash, J.A. Downie, A.E. Senior, F. Gibson, G.B. Cox, Biochem. J. 213 (1983) 451–458.
[59] O.Y. Dmitriev, R.H. Fillingame, J. Biol. Chem. 276 (2001) 27449–27454.
[60] M.E. Girvin, R.H. Fillingame, Biochemistry 33 (1994) 665–674.
[61] F.M. Assadi-Porter, R.H. Fillingame, Biochemistry 34 (1995) 16186–16193.
[62] Y. Zhang, R.H. Fillingame, J. Biol. Chem. 270 (1995) 87–93.
[63] G. Kaim, F. Wehrle, U. Gerike, P. Dimroth, Biochemistry 36 (1997) 9185–9194.
[64] D.L. Foster, R.H. Fillingame, J. Biol. Chem. 257 (1982) 2009–2015.
[65] K. von Meyenburg, B.B. Jorgensen, J. Nielsen, F.G. Hansen, O. Michelsen, Tokai J. Exp. Clin. Med. 7 (1982) 23–31(Supplement).
[66] S.M. Prince, M.Z. Papiz, A.A. Freer, G. McDermott, A.M. Hawthornwaite-Lawless, R.J. Cogdell, N.W. Isaacs, J. Mol. Biol. 268 (1997) 412–423.
[67] N. Grigorieff, T.A. Ceska, K.H. Downing, J.M. Baldwin, R. Henderson, J. Mol. Biol. 259 (1996) 393–421.
[68] L.O. Essen, R. Siegert, W.D. Lehmann, D. Oesterhelt, Proc. Natl. Acad. Sci. U. S. A. 95 (1998) 11673–11678.
[69] P. Dimroth, Biochim. Biophys Acta 1458 (2000) 374–386.
[70] P. Dimroth, G. Kaim, U. Matthey, J. Exp. Biol. 203 (2000) 51–59.
[71] U. Matthey, G. Kaim, D. Braun, K. Wurthrich, P. Dimroth, Eur. J. Biochem. 261 (1999) 459–467.
[72] G. Groth, J.E. Walker, FEBS Lett. 410 (1997) 117–123.
[73] G. Groth, Y. Tilg, K. Schirwitz, J. Mol. Biol. 281 (1998) 49–59.
[74] C. Schnick, L.R. Forrest, M.S.P. Sansom, G. Groth, Biochim. Biophys. Acta 1459 (2000) 49–60.
[75] B. Schulenberg, R. Aggeler, J. Murray, R.A. Capaldi, J. Biol. Chem. 274 (1999) 34233–34237.
[76] O.Y. Dmitriev, R.H. Fillingame, Biochemistry 41 (2002) 5537–5547.
[77] R.H. Fillingame, Science 286 (1999) 1687–1688.